Spectrochimica Acta Part A 79 (2011) 538–547

Contents lists available at ScienceDirect

Spectrochimica Acta Part A: Molecular and Biomolecular Spectroscopy

journal homepage: www.elsevier.com/locate/saa

Solvatochromaticity and pH dependence of the electronic absorption spectra of some purines and pyrimidines and their metal complexes

Mamdouh S. Masoud[a], Medhat A. Shaker[b], Alaa E. Ali[b,*], Gehan S. Elasala[b]

[a] Chemistry Department, Faculty of Science, Alexandria University, Egypt
[b] Chemistry Department, Faculty of Science, Damanhour University, Egypt

ARTICLE INFO

Article history:
Received 3 December 2010
Received in revised form 21 February 2011
Accepted 11 March 2011

Keywords:
Uric
6-Amino-2-thiouracil
Complexes
Solvatochromic
Dissociation constants
pH-effect

ABSTRACT

The solvatochromic responses of uric acid (Ua), 6-amino-2-thiouracil (ATU) and a series of their complexes dissolved in ten solvents of different polarity have been measured. The solvent-dependent UV/Vis spectroscopic absorption maxima, λ_{max}, are assigned to the corresponding electronic transitions and analyzed using SPSS program, regression analysis and Kamlet and Taft methods. The observed solvatochromism is discussed using various solute–solvent interaction mechanisms. The electronic absorption spectra of ATU were investigated in aqueous buffer solutions of varying pH and utilized for the determination of dissociation constants. The ranges of pH, where individual ionic species are predominant have been determined.

1. Introduction

Compounds containing pyrimidine and purine play a significant role in many metabolic processes [1], where both exist in nucleic acids, several vitamins, coenzymes and antibiotics. Attention in our laboratory has escalated regarding the potential of those compounds and their complexes owing to their applicability as potential ligands for a large number of metal ions [2–13]. Compounds containing nitrogen and sulphur as donor atoms such as thiouracil (TU) and 6-amino-2-thiouracil (ATU) have an important role to play as anti-cancer and anti-viral activities [14]. In human species, uric acid (Ua) is one of the final degradation products of purine nucleotides [15]. Accumulation of uric acid in kidneys can lead to severe disorders. More particularly, in cancer patients, cellular disorders or aggressive chemotherapy increase purine metabolism and therefore, the release of large quantities of uric acid in blood. To prevent and cure hyperuricemia, it is common to use a nonhuman proteolytic enzyme, e.g. urate oxidase as a drug to oxidize uric acid [16–18]. In order to elucidate the solvent influence on the spectral behaviour of systems in study, the solvent induced spectral shifts can be related to macroscopic parameters such as the dielectric constant (ε) and with microscopic parameters such as Kamlet and Taft's solvatochromic parameters (α, β, π^*) [19–21], which define the solvent characteristics [22] and evaluate solvent dipolarity/polarizability, solvent hydrogen-bond acidity and solvent hydrogen-bond basicity [23–26]. In this work, the objective is to investigate the solvent influence on the UV/Vis spectral changes of Ua, ATU and some of their complexes: Cr–Ua, Co–Ua, Co–$(Ua)_2$, Co_2–$(Ua)_3$, Ni–Ua, Ni–$(Ua)_2$, Cd–Ua, UO_2–$(Ua)_2$, Na_2–Ua, K–Ua and Cu–$(ATU)_2$. The structures and the abbreviations of the investigated compounds are shown in Fig. 1. The UV–Vis absorption spectra of ATU were investigated in aqueous buffer solutions of varying pH and utilized for the determination of dissociation constants. The ranges of pH, where individual ionic species are predominant have been determined.

2. Experimental

2.1. Materials and methods

2.1.1. Reagents

Uric acid (Fluka, Buchs, Switzerland), 6-amino-2-thiouracil (Sigma, St. Louis, MO) and their complexes have been synthesized by direct combination in basic medium. The solvents used in this study were of HPLC grade (Merck, Darmstadt, Germany) and have been used without further purification. The chemicals used throughout the investigation were of analytical grade quality (Merck). All solutions were prepared with de-ionized and CO_2-free water. The buffer used was of the universal type taking 0.04 M of H_3BO_3, H_3PO_4 and CH_3COOH acids and adding the required volume

* Corresponding author. Tel.: +20 115799866.
E-mail address: dralaae@yahoo.com (A.E. Ali).

1386-1425/$ – see front matter © 2011 Elsevier B.V. All rights reserved.
doi:10.1016/j.saa.2011.03.029

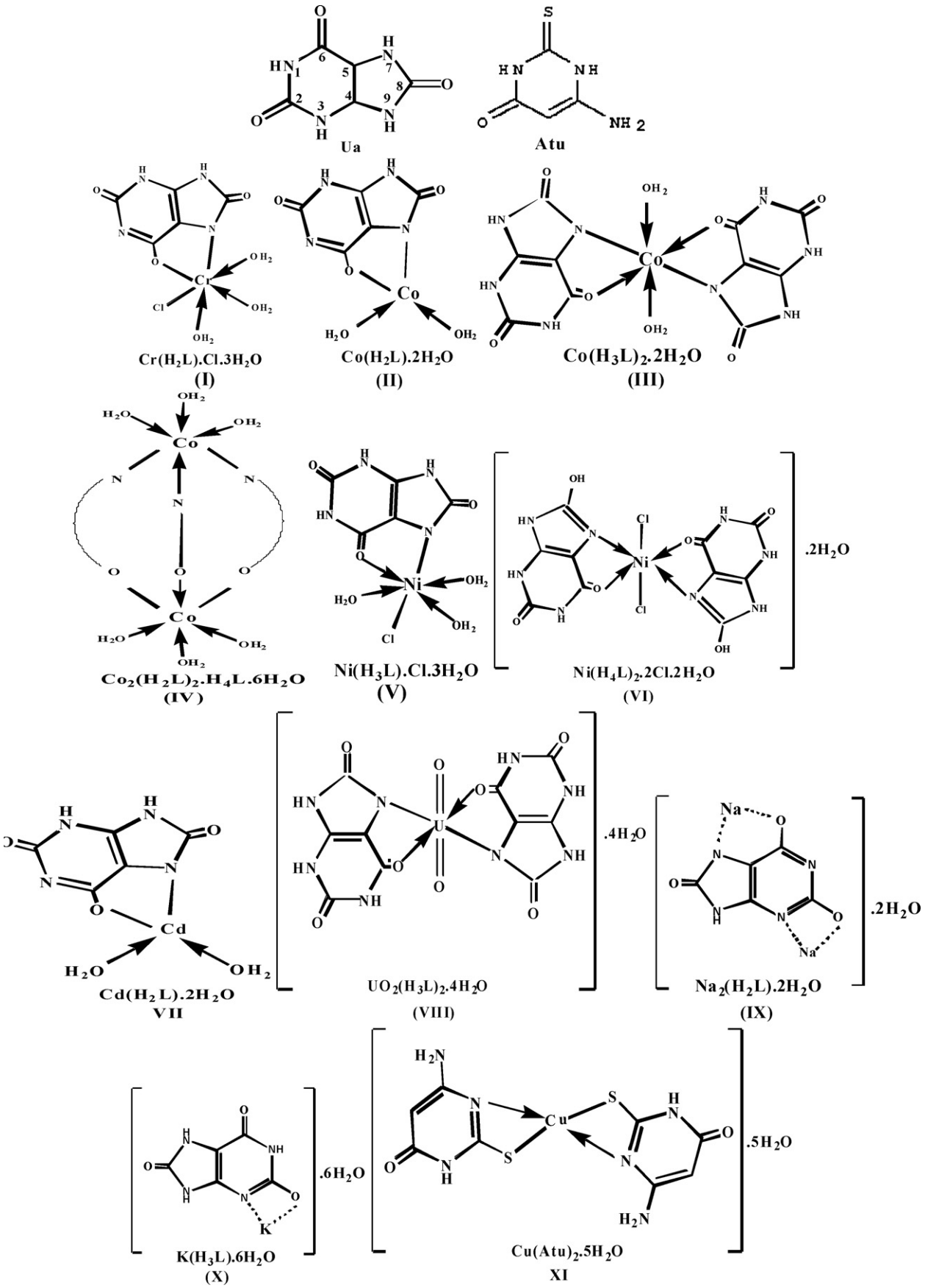

Fig. 1. The structures and the abbreviation of the investigated compounds.

of 0.2 M KOH (CO_2 free) to give the desired pH. A 0.5 M solution of KCl was prepared to adjust the ionic strength of the solutions.

2.1.2. Apparatus

UV–Vis absorbance spectra were recorded with a Perkin-Elmer Lambda 19 spectrophotometer. The pH value was checked using a Cole-Parmer instrument Model 60648 that was previously calibrated with a standard buffer solution of pH's 4.00, 7.00 and 9.18.

2.1.3. Procedure

Electronic absorption spectral measurements were recorded for each investigated compound in the proper solvent. Ten different solvents covering a wide range of solvent parameters, namely ethanol, methanol, *N*,*N*-dimethylformamide (DMF), dimethyl sulfoxide (DMSO), 1,4-dioxane, carbon tetra chloride (CCl_4), acetonitrile, 2-propanol, *n*-butanol and water were used. These solvents have different physicochemical properties, mainly dielectric constant, dipole moment and refractive index. The dissociation constants of ATU were determined by means of the data obtained from spectrophotometric titrations at $37 \pm 0.1\,^{\circ}C$ and $0.15\ mol\,l^{-1}$ ionic strength (NaCl) and pH range 1.5–12.0.

2.2. Data treatment

Different one-, two- and three-parameter equations are applied here using suitable combinations between the solvent polarity parameters *E*, *K*, *J*, *H*, *M* and *N* as reported before [23–25]. The empirical solvent polarity, *E* is sensitive to both solvent–solute hydrogen bonding and dipolar interactions and is related to $\overline{\nu}_{max}$, the wavenumber in cm^{-1} of the absorption maximum of the given solvent as follows [23–25]:

$$E = 1.895 \times 10^{-3}\,\overline{\nu}_{max}$$

The dielectric function of Kirkwood, *K* adequately represents the dipolar dielectric interactions and is a measure of the polarity of the solvent that depends on the dielectric constant of the solvent, *D* [27]:

$$K = \frac{D-1}{2D+1}$$

The function *J* has been introduced to account for non-specific solute–solvent interactions such as dispersion and is related to the dielectric constant of the solvent, *D* [28]:

$$J = \frac{D-1}{D+2}$$

The function *H* has been introduced to account for non-specific solute–solvent interactions such as dipolar effects and is related to the refractive index of the solvent, *n* [28]:

$$H = \frac{n^2-1}{n^2+2}$$

The function *M* has been introduced to account for the solute permanent dipole–solvent induced dipole interactions and is related to the refractive index of the solvent, *n* [29]:

$$M = \frac{n^2-1}{2n^2+1}$$

The function *N* has been introduced to account for the solute permanent dipole–solvent permanent dipole interactions [29]:

$$N = J - H$$

The physical parameters for the solvents at $20\,^{\circ}C$ are collected in Table 1, where *d* is density, *n* is refractive index, *D* is dielectric constant, *R* is molar refraction, μ is dipole moment in Debye and. π^*, α and β are solvatochromic parameters.

In the present work, the observed peak position of an absorption band, *Y* in a given solvent has been expressed as a linear function of different solvent polarity parameters, x_n as follows:

$$Y = a_o + a_1x_1 + a_2x_2 + a_3x_3 + \cdots + a_nx_n$$

The previous equation is amenable to solution for the intercept, a_o and the coefficients, $a_1, a_2, \ldots, a_n$ by multiple regression technique. The regression intercept, a_o has been considered as the peak position in the gas phase spectra [30]. A program of statistical package of social sciences (SPSS) has been used has been used to determine these coefficients by multiple regression technique [23–25]. The residual error, *S*, in a least-squares fits the previous multi-linear equation as follows:

$$S = \sum_{i=1}^{n}(Y_i - a_o - a_1x_{1i} - a_2x_{2i} - a_3x_{3i} - \cdots - a_nx_{ni})^2$$

The least-squares criterion requires that *S* be minimized. This results in sets of equations which can be solved by use of standard matrix methods. The multiple correlation coefficient, *R* or MCC and the probability of variation, *P*, have been considered as a measure of the goodness of the fit.

The solvent induced spectral data were further treated using a two-parameter equation as follows [31]:

$$\nu_{solution} = \nu_{vapour} + K_1\left(\frac{2D-2}{2D+2}\right) + K_2\left(\frac{2n^2-2}{2n^2+1}\right)$$

where $\nu_{solution}$ is the frequency of the peak maximum in the presence of solvent, *D* is the solvent dielectric constant, *n* is the solvent refractive index and ν_{vapour} is the frequency of the peak maximum in the absence of solvent. Multiple regression technique was used to evaluate ν_{vapour}, K_1, K_2 and the correlation coefficients. The third data treatment of the solvent induced spectral shift were carried out using Kamlet and Taft method [32,33]. In this method, the electronic spectroscopic measurement of λ_{max} of a dissolved chromophore provides numerical values for the intermolecular solute–solvent interactions. The effects of solvent polarity and hydrogen bonding on the absorption spectra were interpreted by the linear solvation energy relationships concept developed by Kamlet and Taft using the following general equation:

$$\nu = \nu_o + s\,\pi^* + a\,\alpha + b\,\beta$$

and by a two-parameter, Kamlet and Taft, model represented by the following equation:

$$\nu = \nu_o + s\,\pi^* + a\,\alpha$$

where π^*, α and β are solvatochromic parameters and *s*, *a* and *b* are the solvatochromic coefficients. In these equations, π^* is an index of the solvent dipolarity/polarizability which is a measure of the ability of the solvent to stabilize a charge or a dipole by its own dielectric effects. The π^* scale was selected to run from zero for cyclohexanone to 1.00 for DMSO. The variable α is a measure of the solvent hydrogen-bond donor (HBD) acidity and describes the ability of the solvent to donate a proton in a solvent-to-solute hydrogen bond. The scale α was selected to extend from zero for non-HBD solvents to about 1.00 for methanol. The variable β is a measure of the solvent hydrogen-bond acceptor (HBA) basicity and describes the ability of the solvent to accept a proton in a solute-to-solvent hydrogen bond [34]. The scale β was selected to extend from zero for non-HBD solvents to about 1.00 for hexamethyl phosphoric acid triamide. In these amphiprotic solvents, complications can be caused by self-association type-AB hydrogen bonding and multiple type-A and type-B interactions. In this situation, where both the solvents and the solutes are hydrogen-bond donors, it

Table 1
The physical parameters for the solvents used.

Compound	CCl_4	Dioxane	DMSO	DMF	ACN	Butanol	Isopropanol	Ethanol	Methanol	Water
Dipole moment, μ	0.00	0.45	3.90	3.86	3.84	1.52	1.66	1.69	1.70	1.82
Density, d	1.59	1.034	1.096	0.945	0.79	0.81	0.79	0.789	0.791	0.998
Refractive index, n	1.461	1.422	1.478	1.431	1.34	1.40	1.38	1.361	1.328	1.333
Molar refraction, R	25.8	21.6	20.1	19.9	11.1	22.20	17.5	12.8	8.2	3.7
Dielectric constant, D	2.2	2.2	48.9	36.7	37.5	17.1	18.3	24.3	32.6	78.5
E	32.5	36.0	45.0	43.8	46.0	50.2	48.6	51.9	55.5	63.1
K	0.222	0.223	0.485	0.480	0.480	0.457	0.460	0.470	0.477	0.491
M	0.215	0.203	0.221	0.204	0.175	0.195	0.187	0.181	0.169	0.171
N	0.0117	0.031	0.658	0.666	0.712	0.601	0.622	0.710	0.710	0.757
π^*	0.28	0.55	1.00	0.88	0.75	0.47	0.48	0.54	0.60	1.09
β	0.00	0.37	0.76	0.69	0.31	0.88	0.95	0.77	0.62	0.18
α	0.00	0.00	0.00	0.00	0.19	0.79	0.76	0.83	0.93	1.17

can be quite difficult to untangle solvent dipolarity/polarizability, type-B hydrogen bonding and variable self-association effects from common multiple type-A hydrogen bonding interactions [35]. For the purpose of exploring the solvent effects and hydrogen bonding (types A and B) on the absorption spectra, the absorption frequencies $\bar{\nu}_{max} = 1/\lambda_{max}$ were correlated with the total solvatochromic. The correlation of the spectroscopic data was carried out by means of multiple linear regression analysis.

3. Results and discussions

3.1. Characteristics of solvatochromaticity

The electronic absorption spectra of the investigated compounds were recorded and collected in Table 2. The electronic absorption spectrum of Ua showed the appearance of two distinctive bands. The first band in the range 232–249 nm is assigned as $\pi \rightarrow \pi^*$ due to transitions of conjugated multiple bonds. The other band in the range 280–295 nm is assigned as $n \rightarrow \pi^*$ due to transition of the ketone groups and are expected to take place from non-bonding orbitals to different π^* molecular orbitals [36]. The shorter-wavelength band disappears in dioxane, DMF, DMSO and CCl_4 solvents. The longer-wavelength band appearing in the wavelength range of 280–295 nm is more sensitive band towards the nature of the solvent. For this band, on going from CCl_4 to ACN or *n*-butanol as solvent, a bathochromic shift is observed, while a hypsochromic shift is observed in all other solvents, Table 2. The large positive solvatochromism of the long-wavelength band is in agreement with a distinct $n \rightarrow \pi^*$ of its $S_o \rightarrow S_1$ electronic transition, going from a less dipolar ground to a highly dipolar excited state ($\mu_E > \mu_G$). The electronic spectrum of ATU showed the appearance of $\pi \rightarrow \pi^*$ band in 242–250 nm range, only in the hydroxo-carrying solvents. These high energy bands of $\pi \rightarrow \pi^*$ transitions in these solvents are due to the presence of an external hydrogen bond affecting these absorption bands. The $n \rightarrow \pi^*$ band in the range 280–300 nm appeared in all solvents except CCl_4, Table 2. The longer-wavelength band appearing in the least polar solvent, dioxane, at 280 nm showed a bathochromic shift on increasing the polarity of the solvent. Examining the spectra of Ua complexes (I–XI) shows that the highest energy bands of $\pi \rightarrow \pi^*$ transitions, found in the free ligand, disappeared on complexation for all complexes except VII, IX and X complexes where the linkage of Ua to metal ions is through acidic bonds and not coordinate bond, Fig. 1. The longer-wavelength band, $n \rightarrow \pi^*$ to assign C=O group of the purine or pyrimidine rings is appearing in the spectra of the complexes. The spectral features of the investigated complexes are characterized by the weakness of the bands, the large number of the bands and the great variations in the width of these bands [37]. All these features are easily understood in terms of ligand field theory. The observed d–d transition bands characteristic of these complexes appeared in the range 421–492 nm were assigned as $^3T_{1g}(F) \rightarrow {}^3T_{1g}(P)$ while those appeared in the range 520–630 nm were assigned as $^3T_{1g}(F) \rightarrow {}^3T_{2g}(F)$ [38]. The third spin-allowed transition appeared in the range 630–695 nm. Complexes (I–X) showed four allowed bands in all solvents except water due to complete hydrolysis. Complex VIII showed three allowed bands. Complex XI showed one band in DMSO, DMF and ACN, three bands in isopropanol and two bands in water, methanol, ethanol, butanol and 1,4-dioxane. The $n \rightarrow \pi^*$ transition in most of the complexes has negative solvatochromism (hypsochromic shifts) in polar or hydrogen bonding solvents, whereas a positive solvatochromism (bathochromic shift) was observed in other solvents with respect to its position in the least polar solvent dioxane. The blue shifts may be due to the solute–solvent hydrogen bonding. This leads to the existence of some chromophoric groups, thus the π-system is stabilized and tend to lower the energy of the ground state and thus blue shift occurs with increasing the solvent polarity [39].

DMF is polar aprotic solvent and is known to be strong hydrogen-bond acceptor (HBA), with the highest HBA basicity among most common organic solvents [19,40]. Therefore, the positive solvatochromism may be attributed to the effect of DMF basicity as well as its H-bond accepting character. This indicates that a combination of several solvent characteristics such as polarity, basicity and H-bond-accepting ability is responsible for the spectral characteristics of this complex.

3.2. Regression analysis

The studied regions for Co–UA complex are Y_1 = 290–309 nm, Y_2 = 466–492 nm, Y_3 = 523–555 nm and Y_4 = 630–670 nm. For one parameter regression equation, all MCC values of Y_1, Y_3 and Y_4 regions were very poor while the best correlation coefficients were observed for Y_2 with E (0.729). On the other hand, two-parameter equation showed that the best correlation coefficient was observed for Y_1 and Y_3 with E and N functions. This combination gave higher values of correlations shown by its multiple regression (R) and low probability of variation (P). It is concluded that, the studied properties of the solvent (dielectric constant, refractive index and empirical solvent polarity) are effective parameters to explain the spectral shifts. The best correlation coefficient was observed for Y_2 and Y_4 with the combination N and K functions with MCC = 0.959 and 0.92 for Y_2 and Y_4, respectively. Based on three-parameter regression equation, the best correlation coefficient was observed for Y_1 with E, M, and K functions (MCC = 0.807), for Y_2 with E, N, and K functions (MCC = 0.998), for Y_3 with E, M, and N functions (MCC = 0.985) and for Y_4 with M, N and K functions (MCC = 0.995). The least correlation coefficient was observed with E, M and K functions for Y_2 and Y_4 (MCC = 0.77 and 0.612, respectively). Good regression coefficients obtained from four-parameter regression equation where for Y_1 (MCC = 0.807), for Y_2 (MCC = 0.999), for Y_3 (MCC = 1) and for Y_4 (MCC = 0.998).

Table 2
Electronic absorption spectra of Ua, ATU and their complexes in the presence of different solvents (λ_{max}, nm).

Compound	CCl_4	Dioxane	DMSO	DMF	ACN	*n*-Butanol	Isopropanol	Ethanol	Methanol	Water
Ua	–	–	–	–	240	249	232	238	239	232
	290	280	289	283	295	292	287	290	286	285
ATU	–	–	–	–	–	250	242	248	250	245
	–	280	285	300	282	299	297	300	280	290
I	–	291	297	–	–	293	277	295	294	286
	–	424	429	–	–	425	442	442	434	–
	–	493	477	–	–	491	496	473	471	–
	–	596	584	–	–	562	581	579	582	–
II	–	292	300	–	–	294	309	298	294	290
	–	492	480	–	–	491	482	470	466	–
	–	546	523	–	–	555	528	536	546	–
	–	640	651	–	–	630	643	666	673	–
III	–	294	301	–	–	292	303	300	292	290
	–	455	445	–	–	440	428	452	430	–
	–	541	545	–	–	558	540	535	552	–
	–	675	672	–	–	683	660	680	662	–
IV	–	291	288	–	–	295	292	294	290	290
	–	454	441	–	–	450	462	456	460	–
	–	535	552	–	–	550	537	544	520	–
	–	660	695	–	–	685	685	640	670	–
V	–	290	301	–	–	296	283	300	294	292
	–	421	428	–	–	426	424	425	440	–
	–	540	552	–	–	549	554	565	525	–
	–	658	651	–	–	640	652	632	672	–
VI	–	299	302	–	–	298	282	300	290	290
	–	454	440	–	–	450	458	464	462	–
	–	601	582	–	–	570	587	582	592	–
	–	654	640	–	–	632	654	678	648	–
VII	–	–	–	–	–	–	219	228	241	235
	–	292	291	–	–	296	292	295	291	291
	–	399	–	–	–	401	346	397	399	–
VIII	–	290	291	–	–	287	285	290	292	290
	–	491	470	–	–	490	466	476	450	–
	–	–	–	–	–	–	–	–	–	–
	–	601	604	–	–	600	630	592	628	–
IX	–	–	–	–	–	–	219	240	238	230
	–	294	296	–	–	294	285	296	294	290
	–	398	–	–	–	398	344	–	–	–
X	–	–	–	–	–	–	219	255	237	236
	–	295	292	–	–	296	283	296	294	292
	–	401	–	–	–	399	348	–	–	–
XI	–	–	–	–	–	–	220	260	254	260
	–	290	280	285	278	278	260	291	285	272
	–	397	–	–	–	402	400	–	–	–

3.3. A two-parameter equation model

The data in general pointed that both the dielectric constant and the refractive index of solvents affect the electronic spectral properties of the compounds, but with different degrees. The K_1 and K_2 values are negative, i.e. strong solute–solvent interaction takes place causing a decrease in energy of electronic transition from LUMO to HOMO compared with the vapour state. For all compounds the values of r^2 (υ, D) and r^2 (υ, n) are very poor, Table 3. So, the regression analysis should be applied to find the effect of both functions D and n on the spectral bands. For each compound, the effect of both functions had different degrees. For uric acid, the spectra made using various solvents ($n = 10$) which have different polarities. From the regression, the D function had stronger effect than that of n. So, the peak shifts should depend primarily up on dielectric constant "D". For ATU, the refractive index function had stronger effect than dielectric constant function. So, the peak shifts should depend primarily up on n function. From correlation analysis in all complexes, it seems that the refractive index function had stronger effect than dielectric constant function. So, the peak shifts should depend primarily up on n-function by higher degree than D-function.

3.4. Kamlet and Taft method

The Kamlet–Taft solvatochromic parameters are given in Table 1 [41]. The results of the correlation of the absorption frequencies with the Kamlet–Taft solvatochromic parameters, π^*, α and β, are given in Table 4, and the percentage contribution of the calculated solvatochromic parameters from the values of regression coefficients are given in Table 5 and Fig. 2.

The results show that solvent effects on the absorption spectra of UA, ATU and their complexes generally include important contributions from the solvent hydrogen bond donor (HBD) acidity and the solvent hydrogen bond acceptor (HBA) basicity. It is obvious from the coefficient values that the classic solvation effects, π^* dominate in complex VIII in contrary to the other compounds, where the HBD and HBA effects dominate. The high positive values of the coeffi-

Table 3
K_1 K_2, υ(vapour), and correlation analysis data for ligands and their complexes.

Compound	υ(vapour) (cm^{-1})	K_1	K_2	MCC	r^2 (υ, D)	r^2 (υ, n)
UA	35533.25	−710.95	−475.31	0.301	0.090	0.014
ATU	39148.63	−2399.02	−6821.21	0.428	0.135	0.011
I	411940.24	3792.49	4204.43	0.313	0.000	0.089
II	37791.65	−823.88	−8705.87	0.526	0.015	0.198
V	38624.75	292.28	−12912.73	0.585	0.064	0.337
VII	29265.60	2209.42	8467.81	0.955	0.557	0.104
VIII	34336.24	54.525	494.60	0.062	0.000	0.002
XI	35002.93	2146.33	−2924.98	0.351	0.117	

Table 4
Results of the correlations with Kamlet and Taft model for the investigated compounds.

Compound	υ_0 (10^{-3} cm^{-1})	s (10^{-3} cm^{-1})	b (10^{-3} cm^{-1})	a (10^{-3} cm^{-1})	R	S
UA	34.560	0.409	−0.033	−1.03	0.216	0.64
ATU	37.172	−1.023	−2.702	−0.611	0.664	0.99
II	34.995	−0.59	−1.643	0.405	0.762	0.54
V	33.441	−0.3	0.122	1.038	0.57	0.99
VIII	34.396	−0.27	0.428	0.124	0.602	0.33
I	34.393	−0.45	−0.026	0.589	0.351	1.11
VII	31.727	2.172	1.721	0.071	0.989	0.11
XI	33.402	1.38	1.405	1.016	0.439	1.44

R: correlation coefficient, S: standard error.

Table 5
Percentage contribution of calculated solvatochromic parameters using Kamlet and Taft model.

Compound	s (%)	b (%)	A (%)
UA	27.7853	2.2418	69.9728
ATU	23.5931	62.3155	14.0913
II	22.3654	62.2820	15.3525
V	20.5479	8.3561	71.0958
VIII	32.8467	52.0681	15.0851
I	42.2535	2.4413	55.3051
VII	54.7103	43.5012	1.7884
XI	36.3062	36.9639	26.7298

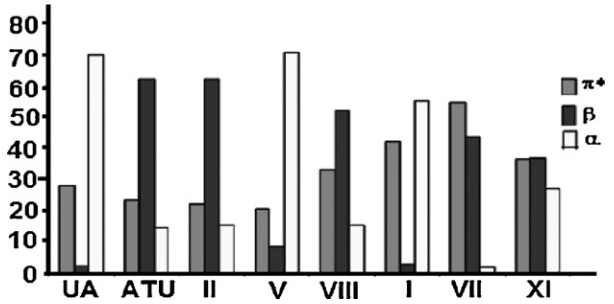

Fig. 2. Contribution of solvatochromic parameters π^*, α and β.

cient, a in complexes I and V indicate a better stabilization of the ground state by the HBD solvent effects and suggest stabilization by the formation of the type A (solvent to solute) hydrogen bonding. The high negative values of the coefficient a in UA indicate a better stabilization of the transition state by the HBD solvent effects due to stabilization by the formation of the type A hydrogen bonding. For ATU and complex II, the solvent hydrogen bond acceptor (HBA) effects dominate with a high negative value so these compounds include important contributions from the HBA basicity. The coefficient values describe the ability of the solvent to accept a proton in solute-to-solvent hydrogen bonding. For complexes VIII and XI, the HBA effects dominate with a high positive value, Table 4. The classic solvation effects, π^* work in the opposite direction to the HBD effects except in ATU, XI and VII and in most cases, their influences are much higher than the influence of the HBD effects. Generally, in most cases the HBA effects, b work in the same direction of the HBD effects. The effects of solvent polarity and hydrogen bonding on the absorption spectra were also interpreted by a two-parameter model, Kamlet and Taft, represented by the following equation: $\nu = \nu_o + s\,\pi^* + a\,\alpha$. The results of the correlations and the percentage contribution of the calculated solvatochromic parameters are given in Tables 6 and 7, and Fig. 3.

The data show that the HBD and the classic solvation effects play a major role to explain the spectral shifts in these compounds. The positive values of HBD effects on Co^{2+}, Ni^{2+}, Cr^{3+} and Cu^{2+} complexes stabilize the ground state by the formation of hydrogen bonding where they act as proton donors. The compounds UA, ATU and VII, Table 6, have the highest positive values for the classic solvation effects while the complex VIII has the highest negative value of the classic solvation effects. The percentages contributions of the calculated solvatochromic parameters, Table 7 and

Table 6
Results of the correlations with the two parameter, Kamlet and Taft, model.

Compound	υ_0 (10^{-3} cm^{-1})	s (10^{-3} cm^{-1})	a (10^{-3} cm^{-1})	R	S
UA	34.543	0.411	−0.108	0.215	0.593
ATU	34.355	0.557	−0.535	0.286	1.156
II	33.198	0.420	0.486	0.416	0.658
V	33.575	−0.375	1.032	0.569	0.856
VIII	34.865	−0.534	0.103	0.499	0.31
I	34.365	−0.434	0.590	0.351	0.96
VII	33.609	1.114	−0.013	0.580	0.493
XI	34.867	0.558	0.976	0.357	1.369

R: correlation coefficient, S: standard error.

Table 7
Percent contribution of the calculated solvatochromic parameters using the two parameter, Kamlet and Taft, model.

Compound	*s* (%)	*a* (%)
UA	79.19075	20.80925
ATU	51.00733	48.99267
II	46.35762	53.64238
V	26.65245	73.34755
VIII	83.83046	16.16954
I	42.38281	57.61719
VII	98.8465	1.153505
XI	36.37549	63.62451

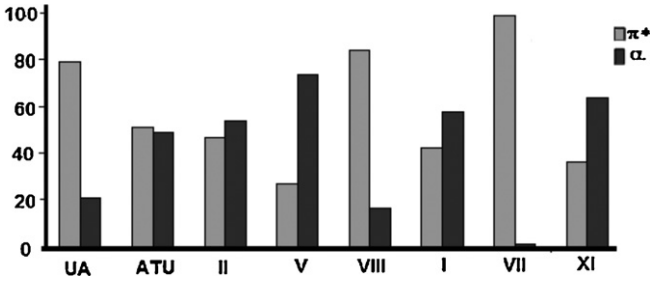

Fig. 3. Contribution of solvatochromic parameters π^* and α using the two parameter, Kamlet and Taft, model.

Fig. 3, show that the HBD and the classic solvation effects have an equal effect in most of the investigated compounds. The correlation coefficients, *R* by applying the equation: $\nu = \nu_o + s\pi^* + a\alpha + b\beta$ have satisfactory values in all cases compared to those obtained by applying the equation: $\nu = \nu_o + s\pi^* + a\alpha$, Table 6. It is known that a negative solvatochromism is induced by increasing the solvent polarity when the ground electronic state is more stabilized compared with the excited and a positive solvatochromism appears in

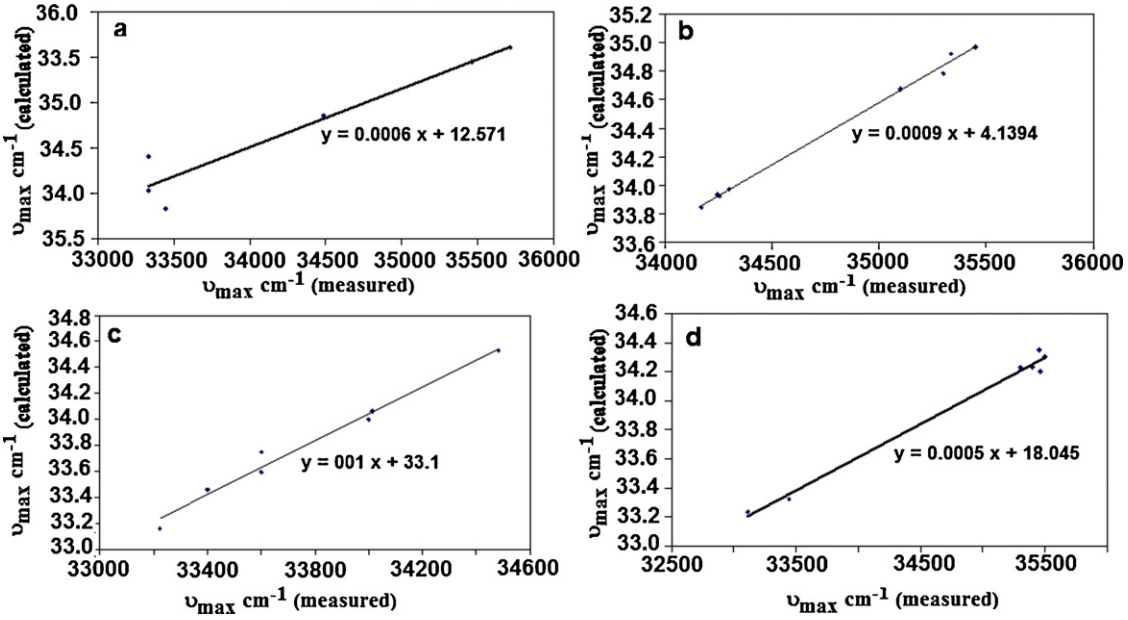

Fig. 4. Linear relationship between the experimental and the calculated absorption maxima ν_{max} (in cm^{-1}) for (a) ATU, (b) UA, (c) II and (d) V.

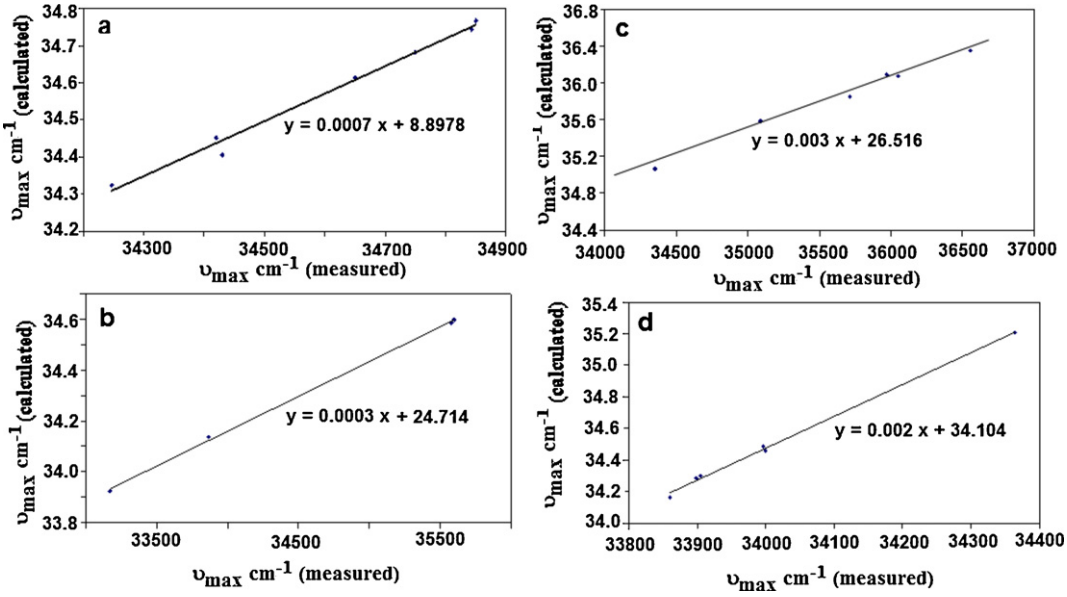

Fig. 5. Linear relationship between the experimental and the calculated absorption maxima ν_{max} (in cm^{-1}) for (a) XIII, (b) I, (c) XI and (d) VII.

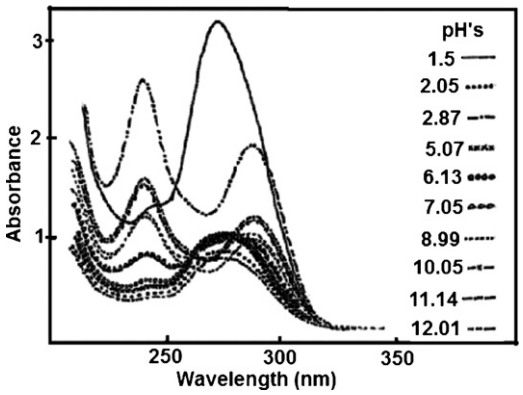

Fig. 6. The electronic spectra of 4×10^{-5} M of ATU at different pH values.

case of higher stabilization of the solute excited state. In order to obtain the magnitude and sign of solvatochromism for each compound, the ν_{max} (maximum wavenumber for the band) in the most polar solvent is subtracted from that determined in the most non-polar solvent, Table 8 and it is considered as a spectral shift, $\Delta\nu$. Positive and negative sign of $\Delta\nu$ are an indicator of the red or blue spectral shifts, respectively [42]. All investigated compounds exhibited a hypsochromic shift (negative solvatochromism) except ATU and VIII compounds, which showed a bathochromic shift (positive solvatochromism) on increasing the solvent polarity, Table 8. This effect was attributed to the interaction of non polar solvents with non-bonding electron pair of nitrogen atom in the investigated compounds [43]. In order to demonstrate the quality of the multi-linear regression analysis, a correlation between the predicted absorbance maxima, ν_{max} calculated from the Kamlet and Taft equation: $\nu = \nu_o + s\pi^* + a\alpha + b\beta$ and the experimental ν_{max} values is shown in Figs. 4 and 5. The linearity of the curves is directly correlated to the multi-linear regression quality.

3.5. Effect of pH on the electronic spectra of ATU and evaluation of its pK_a

When the pH of a solution of ATU is changed, the intensity and position of the absorption band showed pH-dependence and an isosbestic point was observed, presumably, due to the rearrangement of the molecule and the ionization of the hydroxy or mercapto group in position 2 or 4, Fig. 6.

The ionization of hydroxyl group in position 4 is less probable. The formation of an isosbestic point had taken as a proof for the existence of an equilibrium between two absorbing species [44]. The electronic absorption spectra of the compound in the pH range (1.50–12.01) gave two electronic spectral regions: 242–245 nm and 274–288 nm. The first strong band is mainly of the $\pi \rightarrow \pi^*$ type (K band) while the second one is due to $n \rightarrow \pi^*$ transition taking place from non-bonding orbitals of the thiouracil moiety containing N, O and S atoms beside NH_2 group to different π^* molecular orbitals. Different positions are available for the protonation of the groups

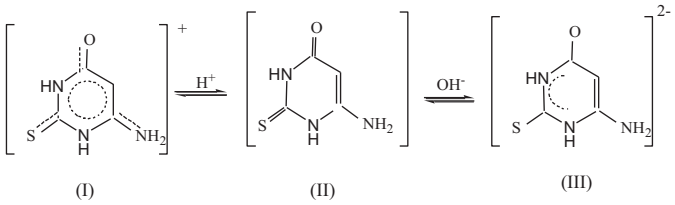

Fig. 7. Cationic (I), neutral (II) and anionic (III) forms of ATU in equilibrium with changing pH of solution.

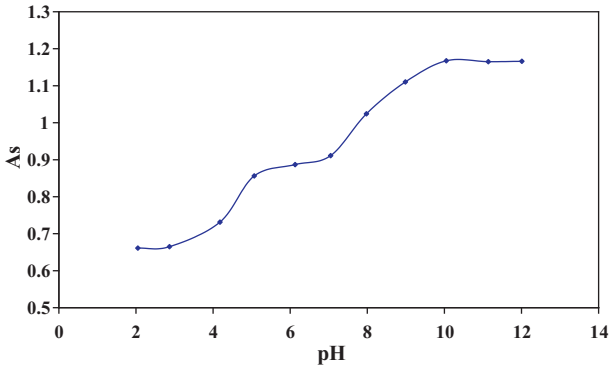

Fig. 8. A_s–pH plot for ATU.

–NH_2, C=O and C=S to give –NH_3^+, C = $\overset{+}{O}$–H and C = $\overset{+}{S}$–H, respectively. The bands are affected with different degrees on increasing the pH values. In the pH range (7.05–12.01), the bands remain at the same position with an increasing in the intensity while in acidic pH range (2.05–6.13), the second band $n \rightarrow \pi^*$ increased in the intensity accompanied with a blue shift. In the same time, the first band $\pi \rightarrow \pi^*$ increased remarkably in intensity with a red shift pointing to the formation of the –SH and –OH auxochrome groups through tautomerism between the [C=S and C=O(4)] and the adjacent [N(1) and N(3)], respectively. For N-heterocyclic mercapto compounds, the spectra [45] resembled those of the N-methyl rather S-methyl derivatives indicating that the mercapto group is present in the thione rather than the thiol form. So, the neutral ATU is likely to exist in the amino-oxo thione form (II), Fig. 7. A great similarity was recorded on measuring the electronic spectra of cytosine and 3-methylcytosine in acidic solutions. So, the resonance hybrid (I), Fig. 7, was chosen to represent the cation of ATU molecule [46]. The spectral data pointed to that ATU gave a slightly red shift in the $n \rightarrow \pi^*$ transition at 242 nm and a marked blue shift in $\pi \rightarrow \pi^*$ transition at 288 nm with the increase in pH and on changing of the neutral form to anionic form. These observations lead to suggest that ATU deprotonation is taking place at N(1) of the nucleus due to the presence of –SH group at position 2 adjacent to N(1) [47].

Different spectrophotometric methods were applied to calculate the pK_a values; the half height [47,48], the modified limiting absorption [49] and Colleter [50] methods, which gave concordant

Table 8
Solvatochromism of UA, ATU and some complexes.

Compound	$(\nu_{max})_{most\ non\text{-}polar\ solvent}$ (10^3 cm^{-1})	$(\nu_{max})_{most\ polar\ solvent}$ (10^3 cm^{-1})	$\Delta\nu$ (10^3 cm^{-1})	Solvatochromism
UA	34.48	35.09	−1.42	–
ATU	35.71	34.48	1.23+	+
II	34.01	34.48	−0.47	–
V	33.44	34.48	−1.04	–
VIII	34.48	34.25	+0.23	+
I	34.36	34.96	−0.6	–
VII	34.25	34.36	−0.11	–
XI	34.48	36.76	−2.28	–

Table 9
pK_a values of ATU (0.5 M KCl, 25 °C).

pK's values								Number of ionized protons (n)		λ (nm)	Isosbestic points (nm)
Half height		Modified limiting absorption		Colleter		Average values					
pK_{a1}	pK_{a2}	pK_{a1}	pK_{a1}	pK_{a1}	pK_{a1}	pK_{a1}	pK_{a1}	n_1	n_1		
4.5	8.0	4.4	8.0	4.6	7.79	4.5 ± 0.1	8.0 ± 0.12	1	1	288	242,265,280

results, Table 9. In the half-height method the pK values were evaluated at constant wavelength from the half-height of the absorbance, A_s versus pH curves, Fig. 8, where pK_a = pH at the half height of the curve.

In the modified limiting absorption method, Fig. 9, the pK_a values were evaluated by applying the following equation:

$$\mathrm{pH} = \mathrm{p}K_a + \log\gamma + \log\frac{A_s - A_{s_{min}}}{A_{s_{max}} - A_s}$$

where $A_{s_{max}}$ is the maximum absorption, $A_{s_{min}}$ is the minimum absorption, A_s is the absorption at any pH and γ is activity coefficient term. By plotting the log absorbance ratio versus pH, a straight line was obtained with a slope giving the number of ionized protons. When log absorbance ratio term equals zero, pK_a = pH.

Finally, in the Colleter method, the pK_a values were evaluated, where three different concentrations of hydrogen ions were selected and their absorbance values were given, $[H^+]_1 > [H^+]_2 > [H^+]_3$ and $A_1 > A_2 > A_3$. The acid dissociation constant is calculated:

$$K = \frac{[H^+]_2 - M[H^+]_3}{M - 1}$$

$$M = \frac{A_3 - A_1}{A_2 - A_1}\cdot\frac{[H^+]_1 - [H^+]_2}{[H^+]_1 - [H^+]_3}$$

Reported data for uracil gave two pK_a values, pK_{a1} of 9.0 at 258 nm with the liberation of two protons through ionization, probably due to the removal of a proton from the N_1=C_2–OH and the pK_{a2} value of 12 with the liberation of a proton from N_3=C_4–OH [51] while 6-amino uracil gives one pK_a value, Fig. 10.

The ionization constants obtained for ATU, Table 9 and Fig. 6 were 4.50 and 8.0 and three isosbestic points appeared at 242, 265

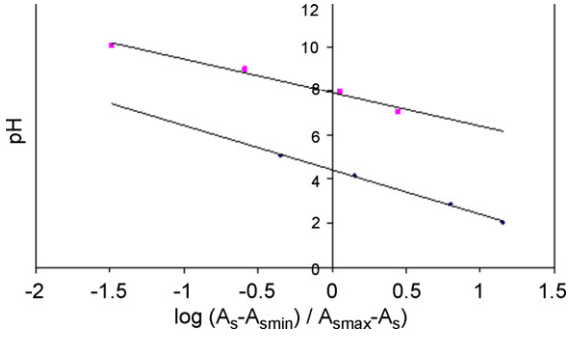

Fig. 9. Modified limiting absorption plot for ATU.

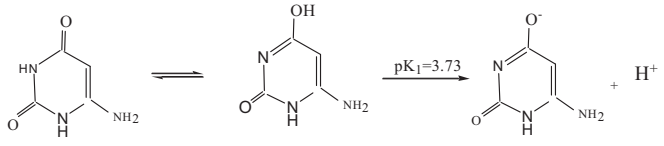

Fig. 10. pK_a value of 6-amino uracil gives.

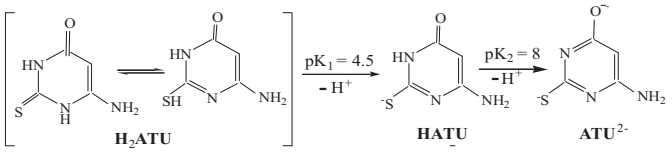

Fig. 11. The proposed mode of ionization of ATU.

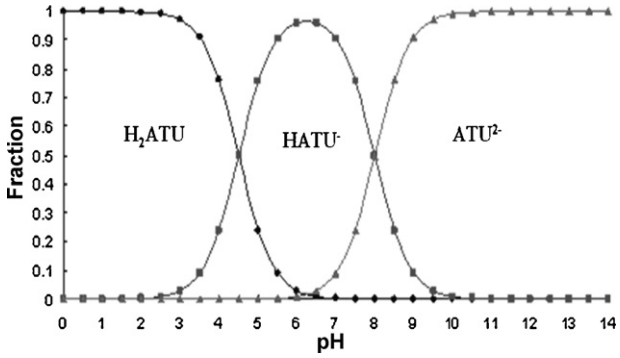

Fig. 12. Concentration distribution diagram for protonated species of ATU.

and 280 nm. The mode of ionization is proposed to be as shown in Fig. 11.

3.5.1. *Distribution of species at different pH values*

In the distribution diagrams, a plot the fraction of an acid species versus how that fraction varies with pH was made, Fig. 12. The variation of the species is due to the acid dissociation shifting as pH changes [52]. ATU has two pK values (4.5 and 8.0) and thus is considered as a diprotic acid. The concentration distribution diagram shows that the ligand is fully protonated giving H_2 ATU species at pH 2.5. Upon increase of pH the concentration of this species decreases and the monoprotonated species $HATU^-$ starts to form and reaches its maximum concentration of 100% in the pH range 6.0–6.5. On further increase of pH the concentration of the monoprotonated species decreases and the unprotonated species ATU^- starts to form and reaches its maximum concentration of 100% in the pH ≥10. It is concluded that the presence of the three species varied as pH changes. In acidic medium, the predominant species is H_2ATU, in basic medium, the predominant species was ATU^{2-} and in the neutral medium the predominant species was $HATU^-$. This means that in basic solution H_2ATU liberates two protons from N(1)=C(2)–SH and N(3)=C(4)–OH and in neutral solution H_2ATU liberates one proton only from N(1) to give N(1)=C(2)–SH.

References

[1] F. Hueso, N.A. Illán, M.N. Moreno, J.M. Martínez, M.J. Ramírez, J. Inorg. Biochem. 94 (2003) 326–334.
[2] M.S. Masoud, M.K. Awad, M.A. Shaker, M.M.T. El-Tahawy, Corros. Sci. 52 (2010) 2387–2396.
[3] M.S. Masoud, M.F. Amira, A.M. Ramadan, G.M. El-Ashry, Spectrochim. Acta 69A (2008) 230–238.

[4] M.S. Masoud, E.A. Khalil, A.M. Ramadan, Y.M. Gohar, A. Sweyllam, Spectrochim. Acta 67A (2007) 669–677.
[5] M.S. Masoud, E.A. Khalil, A.M. Hindawy, A.E. Ali, E.F. Mohamed, Spectrochim. Acta 60A (2004) 2807–2817.
[6] M.S. Masoud, S.A. Abou El-Enein, O.F. Hafez, J. Therm. Anal. 38 (1992) 1365–1376.
[7] M.S. Masoud, S.S. Haggag, Z.M. Zaki, M. El-Shabasy, Spectrosc. Lett. 27 (1994) 775–786.
[8] M.S. Masoud, A.A. Hasanein, A.K. Ghonaim, E.A. Khalil, A.A. Mahmoud, Z. Phys. Chem. 209 (1999) 223–228.
[9] M.S. Masoud, S.A. Abou El-Enein, N.A. Obeid, Z. Phys. Chem. 215 (2001) 867–872.
[10] M.S. Masoud, S.A. Abou El-Enein, H.M. Kamel, Indian J. Chem. 41A (2002) 297–301.
[11] M.S. Masoud, A.Kh. Ghonaim, R.H. Ahmed, S.A. Abou El-Enein, A.A. Mahmoud, J. Coord. Chem. 55 (2002) 79–105.
[12] M.S. Masoud, S.A. Abou El-Enein, M.E. Ayad, A.S. Goher, Spectrochim. Acta 60A (2004) 70–87.
[13] M.S. Masoud, E.A. Khalil, A.M. Hafez, A.F. El-Husseiny, Spectrochim. Acta 61A (2004) 989–993.
[14] R.M. Izatt, J.H. Christensen, J.H. Rytting, Chem. Rev. 72 (1971) 439–481.
[15] D. Voet, J.G. Voet, Biochemistry, 3rd ed., Wiley, New York, 2004.
[16] C. Ronco, P. Inguaggiato, V. Bordoni, M. De Cal, M. Bonello, E. Andrikos, Y. Assuman, R. Rattanarat, R. Bellomo, Contrib. Nephrol. 147 (2005) 115–123.
[17] B.D. Cheson, B.S. Dutcher, J. Support Oncol. 3 (2005) 127–128.
[18] A.M. Tsimberidou, M.J. Keating, Contrib. Nephrol. 147 (2005) 47–60.
[19] M.J. Kamlet, R.W. Taft, J. Am. Chem. Soc. 98 (1976) 377–383.
[20] M.J. Kamlet, J.L. Abboud, R.W. Taft, J. Am. Chem. Soc. 99 (1977) 6027–6038.
[21] M.J. Kamlet, J.L. Abboud, R.W. Taft, in: R.W. Taft (Ed.), Progress in Physical Organic Chemistry, vol. 13, Interscience, New York, 1981, p. 445.
[22] I. Marqués, G. Fonrodona, S. Butĭı, J. Barbosa, Trends Anal. Chem. 18 (1999) 72–76.
[23] M.S. Masoud, A.E. Ali, M.A. Shaker, M. Abdul Ghani, Spectrochim. Acta 61A (2005) 3102–3107.
[24] M.S. Masoud, A.E. Ali, M.A. Shaker, M. Abdul Ghani, Spectrochim. Acta 60A (2004) 3155–3159.
[25] M.A. Khalifa, M.A. Shaker, Alex. J. Pharm. Sci. 9 (1995) 159–161.
[26] I. Marqués, G. Fonrodona, A. Baró, J. Guiteras, J.L. Beltrán, Anal. Chim. Acta 471 (2002) 145–158.
[27] J.G. Kirkwood, J. Chem. Phys. 2 (1934) 351–361.
[28] G. David, H.E. Hallam, Spectrochim. Acta 23A (1967) 593–603.
[29] E.G. McRae, J. Phys. Chem. 61 (1957) 562–572.
[30] L.J. Hilliard, D.S. Foulk, H.S. Gold, Anal. Chim. Acta 133 (1981) 319–327.
[31] H.H. Hammud, A.M. Ghannoum, F.A. Fares, L.K. Abramian, K.H. Bouhadir, J. Mol. Struct. 881 (2008) 11–20.
[32] N. Trišović, N. Banjac, N. Valentić, J. Sol. Chem. 38 (2009) 199–208.
[33] M.J. Kamlet, J.L. Abbould, R.W. Taft, Phys. Org. Chem. 13 (1981) 485–630.
[34] M. Eto, O. Tajiri, H. Nakagawa, K. Harano, Tetrahedron 54 (1998) 8009–8014.
[35] V. Stamatovska, V. Dimova, K. Čolančeska-Raġenovik, Bull. Chem. Technol. Maced. 25 (2006) 9–20.
[36] O.V. Kovalchukova, R.K. Gridasova, B.E. Zaitsev, Z. Neorg. Khim. 26 (1981) 985–989.
[37] K. Jǿrgensen, Absorption Spectra and Chemical Bonding in Complexes, Pergamon Press, 1962.
[38] A.B.P. Lever, Inorganic Electronic Spectroscopy, 2nd ed., Elsevier, Amsterdam, 1984.
[39] T.S. Basu Baul, T.K. Chattopadhyay, B. Majee, Polyhedron 2 (1983) 635–640.
[40] M.J. Kamlet, J.L.M. Abboud, M.H. Abraham, R.W. Taft, J. Org. Chem. 48 (1983) 2877–2887.
[41] G.S. Uscmlic, J.B. Nikolic, V.V. Krstic, J. Serb. Chem. Soc. 67 (2002) 353–359.
[42] E. Rusu, D.O. Dorohoi, A. Airinei, J. Mol. Struct. 887 (2008) 216–219.
[43] M. El-Sayed, H. Muller, G. Rheinwald, S. Spange, Chem. Mater. 15 (2003) 746–751.
[44] M.D. Cohen, E. Fisher, J. Chem. Soc. (1962) 3044–3052.
[45] A. Albert, G.B. Barlin, J. Chem. Soc. (1959) 2384–2396.
[46] E.S. Raper, R.E. Oughtred, I.W. Nowell, Acta Crystallogr. C 41 (1985) 758–760.
[47] M.S. Masoud, H.H. Hammud, H. Beidas, Thermochim. Acta 381 (2002) 119–131.
[48] R.M. Issa, J. Chem. UAR 14 (1971) 113–124.
[49] A.A. Muk, M.B. Pravica, Anal. Chim. Acta 45 (1969) 534–538.
[50] J.C. Colleter, Ann. Chim. 5 (1960) 415–419.
[51] M.M. Taquikham, C.R. Krishnamorthy, J. Inorg. Nucl. Chem. 36 (1974) 711–716.
[52] A.A. Shoukry, M.M. Shoukry, Spectrochim. Acta 70A (2008) 686–691.